OXFORD
SOT | Society of Toxicology
www.toxsci.oxfordjournals.org

TOXICOLOGICAL SCIENCES, 141(1), 2014, 132–140

doi: 10.1093/toxsci/kfu112
Advance Access Publication Date: June 12, 2014

Toxicity of Nanoparticles Embedded in Paints Compared with Pristine Nanoparticles in Mice

Stijn Smulders*, Katrien Luyts*, Gert Brabants†, Kirsten Van Landuyt‡, Christine Kirschhock†, Erik Smolders§, Luana Golanski¶, Jeroen Vanoirbeek*, and Peter HM Hoet*,[1]

*Center for Environment and Health, KU Leuven, Leuven, Belgium, †Centre for Surface Chemistry and Catalysis, KU Leuven, Leuven, Belgium, ‡KU Leuven BIOMAT, Department of Oral Health Sciences, KU Leuven, Leuven, Belgium, §Division of Soil and Water Management, KU Leuven, Leuven, Belgium and ¶CEA-Grenoble, Liten, 17 rue des Martyrs, France

[1]To whom correspondence should be addressed. Fax: +32 16 33 08 06. E-mail: peter.hoet@med.kuleuven.be.

ABSTRACT

The unique physical and chemical properties of nanomaterials have led to their increased use in many industrial applications, including as a paint additive. For example, titanium dioxide (TiO_2) engineered nanoparticles (ENPs) have well-established anti-UV, self-cleaning, and air purification effects. Silver (Ag) ENPs are renowned for their anti-microbial capabilities and silicon dioxide (SiO_2) ENPs are used as fire retardants and anti-scratch coatings. In this study, the toxic effects and biodistribution of three pristine ENPs (TiO_2, Ag, and SiO_2), three aged paints containing ENPs (TiO_2, Ag, and SiO_2) along with control paints without ENPs were compared. BALB/c mice were oropharyngeally aspirated with ENPs or paint particles (20 μg/aspiration) once a week for 5 weeks and sacrificed either 2 or 28 days post final aspiration treatment. A bronchoalveolar lavage was performed and systemic blood toxicity was evaluated to ascertain cell counts, induction of inflammatory cytokines, and key blood parameters. In addition, the lung, liver, kidney, spleen, and heart were harvested and metal concentrations were determined. Exposure to pristine ENPs caused subtle effects in the lungs and negligible alterations in the blood. The most pronounced toxic effects were observed after Ag ENPs exposure; an increased neutrophil count and a twofold increase in pro-inflammatory cytokine secretion (keratinocyte chemoattractant (KC) and interleukin-1ß (IL-1ß)) were identified. The paint containing TiO_2 ENPs did not modify macrophage and neutrophil counts, but mildly induced KC and IL-1ß. The paints containing Ag or SiO_2 did not show significant toxicity. Biodistribution experiments showed distribution of Ag and Si outside the lung after aspiration to respectively pristine Ag or SiO_2 ENPs. In conclusion, we demonstrated that even though direct exposure to ENPs induced some toxic effects, once they were embedded in a complex paint matrix little to no adverse toxicological effects were identified.

Key words: nanotoxicology; occupational health; *in vivo*; mice; inhalation toxicology

Current applications of engineered nanoparticles (ENPs) cover a wide range of industrial and consumer sectors including cosmetics, medicines, and material sciences (Som *et al.*, 2011). In the field of constructions, ENPs can improve vital material characteristics such as increased strength and durability while decreasing the overall weight. ENPs have also been shown to add useful properties to materials including thermal, self-cleaning, and antifogging effects (Lee *et al.*, 2010). ENPs have also shown tremendous potential as a paint additive in the development of new coating and paint systems for wood, metals, ceramics, natural stone, concrete, composites, and plastics (Hanus and Harris, 2013). In terms of industrial applications, coatings, paints, and pigments are the most important applications of ENPs in terms of overall use (Keller *et al.*, 2013).

Three of the most prevalent ENPs used in paints and coatings are titanium dioxide (TiO_2), silver (Ag), and silicon dioxide

(SiO_2) (Hanus and Harris, 2013). A study of Mueller and Nowack in 2008 showed that 35% of the nano-Ag production and 25% of the nano-TiO_2 production in Europe are used by the paint and coating industry, making this sector the first end user of nano-Ag and the second end user of nano-TiO_2 (Mueller and Nowack, 2008). The photocatalytic and hydrophobic properties of nano-TiO_2 give rise to coatings with self-cleaning, air purifying, and anti-UV properties. Nano-Ag replace chemical biocides for antimicrobial efficiency, whereas addition of nano-SiO_2 will increase the scratch and fire resistance of paints and coatings (Chantarachindawong *et al.*, 2012; Lee *et al.*, 2010). Examples of other ENPs currently being used in paints and coatings are zinc oxide (ZnO) due to its self-cleaning and anti-UV properties, and carbon nanotubes for their fire resistance and increased tensile strength.

Occupational exposure to ENPs used in paints and coatings can occur both during the production process or when the coating is applied. Inhalation of aerosols is the most probably route of exposure, especially when coatings are applied by spray applications as typically done in the paint industry. Exposure post coating can also occur due to ageing processes such as UV exposure, thermal stress, water damage and scratching or during the removal process, which includes sanding and drilling. Kaegi *et al.* and Vorbau *et al.* observed that the particles are not released as single ENPs, but rather are released part of a larger matrix particles containing both the ENPs and the coating substrate (Kaegi *et al.*, 2008; Vorbau *et al.*, 2009). Furthermore, indoor exposure is expected to be higher compared with outdoor exposure, due to smaller spaces and lack of proper ventilation.

Toxic effects of ENPs are well defined and have been a major research focus over the past few years. Yet, not much is known about their toxicity when they are embedded in a complex paint or coating matrix. In this study, the inflammatory and toxic effects of three pristine ENPs (TiO_2, Ag, and SiO_2), three aged paints containing ENPs (TiO_2, Ag, and SiO_2) along with control paints without ENPs were compared. Mice were pulmonary exposed by oropharyngeal aspiration and both local (lung) as systemic inflammation were evaluated. Furthermore, the biodistribution of the pristine ENPs and aged paints containing ENPs to different organs (lung, kidney, spleen, liver, and heart) was assessed by inductively coupled plasma mass spectrometry (ICP-MS). Our results indicate that while exposure to pristine ENPs does induce a toxic response, the incorporation of ENPs in a paint matrix blocked most of the particle-induced toxicity.

MATERIALS AND METHODS

Materials

Pristine ENPs (TiO_2, Ag, and SiO_2), paints containing these ENPs, and control paints without ENPs were provided by industrial project partners. An overview of the composition of the different non-aged liquid paints and control paints is shown in Supplementary table 1. Isoflurane (Forene) was obtained from Abbott Laboratories (S.A. Abbott N.V., Ottignies, Belgium) and pentobarbital (Nembutal) from Sanofi Santé Animale (CEVA, Brussels, Belgium).

Manufacturing Aged Powder Paint Particles

Liquid paints were applied on plastic panels using a film applicator creating a uniform film of 200 μm thickness. After drying for 24 h at room temperature (20°C), paints were removed manually using a metallic spatula to obtain powder paints. These powders were milled using a planetary ball mill PM 100 (Retsch, Haan, Germany) and finally exposed to UV-A (Philips TL20W/09N) for 500 h (64 cycles with lamps switched on for 4 and 4 h with lamps switched off) as an ageing process.

Particle Characterization

Scanning electron microscopy. The aged paint powders were deposited on aluminum stubs covered with self-adhesive carbon tabs (G3347N, Agar Scientific, Essex, UK). After gold-sputtering, the paint particles were characterized by scanning electron microscopy (SEM) (Jeol JSM-6610 LV, accelerating voltage: 10 kV, working distance: 10 mm).

Dynamic light scattering. Multiangle dynamic light scattering (DLS) measurements were carried out on an ALV/CGS 3 instrument (ALV, Langen, Germany). In order to avoid any possible contaminations, the capillaries were cleaned with filtered acetone (450 nm Chromafil PTFE filters) and dried at 110°C prior to measurements. Samples were put in the ultrasound bath for 15 min and inserted 5 min before measurement to allow for temperature stabilization. Several sets of 60 s DLS measurements were performed at scattering angles ranging from 30° to 150° in steps of 15°, with a wavelength of 632.8 nm. This multiangle approach will allow to correct for the angular dependence of the scattered intensity, which results from particle anisotropy and/or polydispersity. Modeling of the intensity autocorrelation functions was performed using the cumulant method (whenever applicable) and cross-checked with the maximum entropy method.

Zeta potential. Zeta potential measurements were carried out on a ZetaPlus zeta potential analyser (Brookhaven Instruments, Holtsville), extended with the ZetaPALS option. The PALS (Phase Analysis Light Scattering) is more sensitive than the Doppler method used in the basic ZetaPlus setup. The samples for zeta potential measurements were recovered after DLS measurements and the obtained results were analyzed using the Smoluchowski model.

Mice

Male BALB/c OlaHsd mice (6 weeks old) were obtained from Harlan (Horst, The Netherlands). The mice were housed in a conventional animal house with 12-h dark/light cycles. They were housed in filter top cages and received lightly acidified water and pelleted food (Trouw Nutrition, Ghent, Belgium) *ad libitum*. All experimental procedures were approved by the local Ethical Committee for Animal Experiments.

Experimental Protocol

On days 0, 7, 14, 21, and 28, mice received under light isoflurane anesthesia an oropharyngeal aspiration (25 μl) of pristine ENPs, aged paint particles containing ENPs, control aged paint particles (0.8 mg/ml), or vehicle (saline (0.9% NaCl)). Mice were sacrificed by an intraperitoneal injection of pentobarbital (90 mg/kg body weight) 2 days post final aspiration treatment (day 30). A second group of mice exposed to pristine ENPs or vehicle was sacrificed 28 days post final aspiration treatment (day 56). A schematic overview of the experimental protocol is shown in Figure 1.

Pulmonary Inflammation (Bronchoalveolar Lavage)

The bronchus of the left lung was clamped off before lavaging the right lung, *in situ*, three times with 0.4 ml sterile saline (0.9% NaCl), and the recovered fluid was pooled. Total cells were counted using a Bürker hemocytometer and the bronchoalveolar lavage (BAL) fluid was centrifuged (1000 g, 10 min). Lactate dehydrogenase was determined in the supernatant by spectropho-

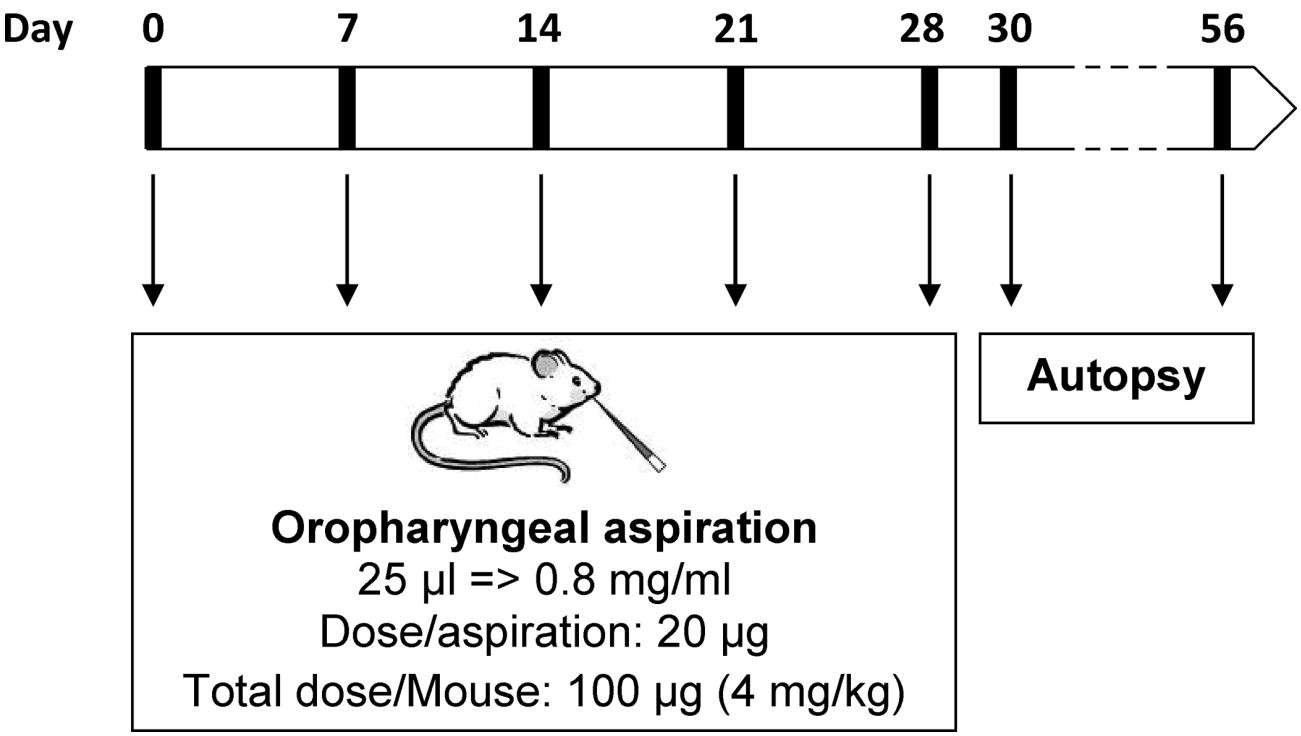

FIG. 1. Schematic overview experimental design. Mice are exposed to the different particles on day 0, 7, 14, 21, and 28 by oropharyngeal aspiration under light isoflurane anesthesia. An autopsy was performed on day 30 or 56.

tometrically monitoring the reduction of pyruvate (Napierska *et al.*, 2009), the remaining supernatant was frozen (−80°C) until further analysis. For cell counts of leukocyte subpopulations, 250 µl of the resuspended pellets (100,000 cells/ml) was spun (300 g, 6 min) (Cytospin 3, Shandon, TechGen, Zellik, Belgium) onto microscope slides, air-dried, and stained (Diff-Quik method, Medical Diagnostics, Düdingen, Germany). For each sample, 200 cells were counted for the number of macrophages and neutrophils. Following thawing of the frozen supernatant, total protein levels were determined using the Bio-Rad Protein assay, according to the Bradford method (Bio-Rad Laboratories GmbH, München, Germany).

Cytokines. Two pieces of the left lung lobe were removed, snap frozen in liquid nitrogen and stored at −80°C until further analysis. Inflammatory cytokines (interleukin-1ß (IL-1ß), IL-12p70, IFN-γ, IL-6, keratinocyte chemoattractant (KC), IL-10, and TNF-α) were measured in homogenized lung tissue with the Mouse ProInflammatory 7-Plex Ultra-Sensitive Kit (Meso Scale Discovery, Gaithersburg), according to the manufacturer's instructions.

Metal concentrations. Ti, Ag, and Si concentrations were measured in the other lung piece, kidney, spleen, liver, and heart by ICP-MS. One milliliter of nitric acid (HNO_3) 60% ultrapur (Merck, Darmstadt, Germany) was added to ∼30 mg tissue or 3–4 mg paint particles and heated at 140°C for 5 h. Finally, samples were diluted in Milli-Q water to 10 ml and Ti, Ag, and Si concentrations were measured by ICP-MS (Agilent 7700x ICP-MS). Elements were measured as ^{47}Ti, ^{107}Ag, and ^{28}Si using Ge and Rh as internal standards. The limits of quantification in the solutions were 0.15 µg/l (Ag and Ti) or 15 µg/l (Si).

Systemic Inflammation (Blood Parameters)
Blood was collected from the retro-orbital plexus. Blood cell counts and differentials were performed on a Cell-Dyn 3500R counter (Abbott, Diegem, Belgium). Plasma samples, obtained after centrifugation (14,000 g, 10 min) of whole blood, were stored at −80°C until further analysis. Inflammatory cytokines (IL-1ß, IL-12p70, IFN-γ, IL-6, KC, IL-10, and TNF-α) were measured in plasma with the Mouse ProInflammatory 7-Plex Ultra-Sensitive Kit (Meso Scale Discovery, Gaithersburg), according to the manufacturer's instructions.

Data Analysis
All data are presented as means and standard deviations (SD). All data were analyzed using the non-parametric Kruskal-Wallis test followed by a Dunn's multiple comparison test (Graphpad Prism 4.01, Graphpad Software Inc., San Diego). A level of $p<0.05$ was considered significant.

RESULTS

A detailed characterization of all pristine ENPs has been published earlier by Smulders *et al.* (2012). Shortly, transmission electron microscopy analysis showed average particle sizes of 15 nm (TiO_2), 25–85 nm (Ag), and 19 nm (SiO_2). DLS analysis showed single populations of 396 nm (TiO_2), 90 nm (Ag), and 192 nm (SiO_2). A selection of SEM images of the aged paint particles containing ENPs and control paints is shown in Figure 2. All paints show a very heterogeneous composition, showing both large (>10 µm) and smaller particles (<1 µm). Smaller particles are mostly found in aggregates with other small particles or attached on the surface of larger particles. Hydrodynamic size and zeta potential of all paint particles are presented in Table 1. The elemental composition of the different aged paint particles and aged control paints, analyzed by ICP-MS, is shown

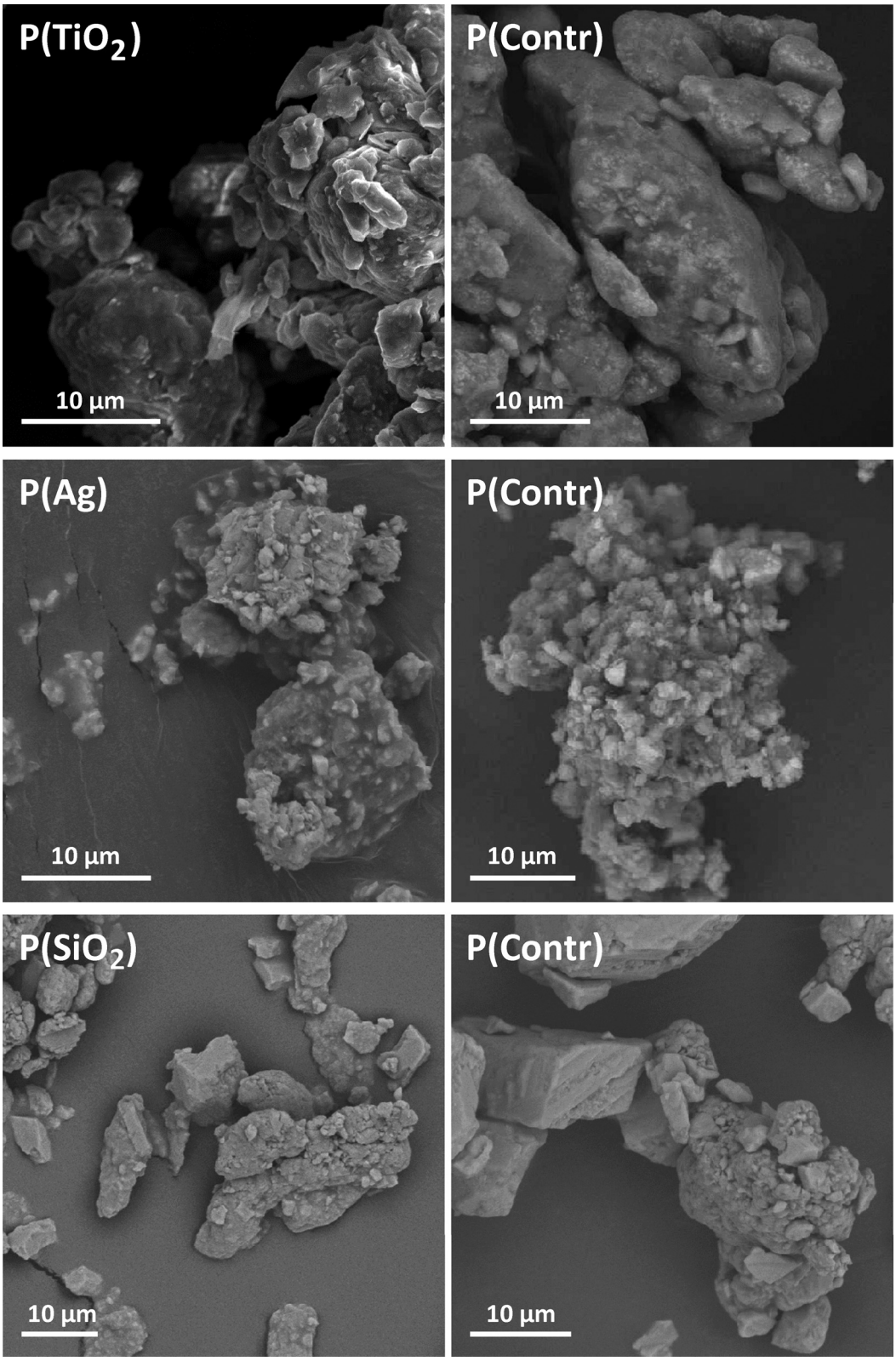

FIG. 2. Electron microscope images of the different aged paint particles. Images of aged paint particles containing TiO_2, Ag, or SiO_2 ENPs (left graphs) and control paint particles without ENPs (right graphs) were obtained by SEM.

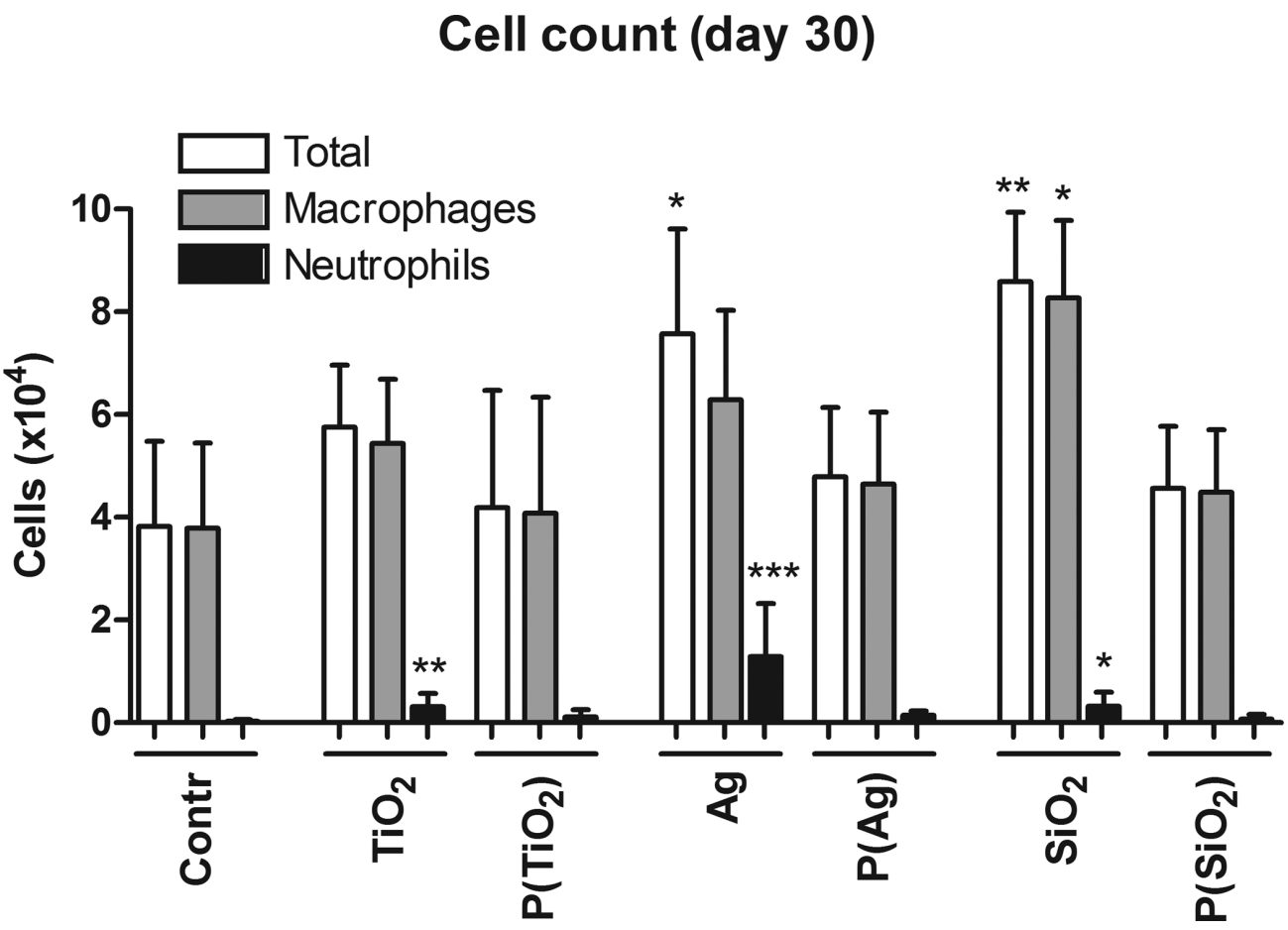

FIG. 3. BAL cell counts at day 30 of mice exposed to pristine ENPs or aged paint particles. Mice were exposed to pristine ENPs (TiO_2, Ag, or SiO_2) or to aged paints containing TiO_2 (P(TiO_2)), Ag (P(Ag)), or SiO_2 (P(SiO_2)). Total and differential (macrophages and neutrophils) cell counts were performed in the BAL fluid. Mean±SD, $n = 4$. $^*p<0.05$, $^{**}p<0.01$, $^{***}p<0.001$ compared with control (saline (0.9% NaCl)).

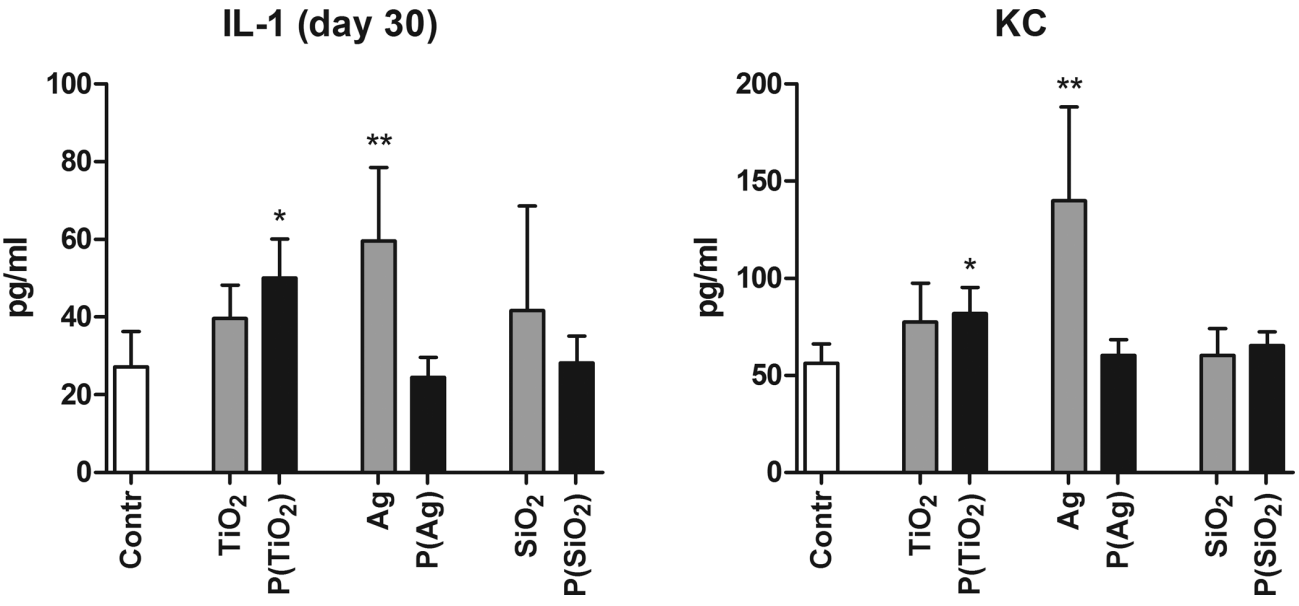

FIG. 4. IL-1 and KC in lung tissue at day 30 of mice exposed to pristine ENPs or aged paint particles. Mice were exposed to pristine ENPs (TiO_2, Ag, or SiO_2) or to aged paints containing TiO_2 ENPs (P(TiO_2)), Ag ENPs (P(Ag)), or SiO_2 ENPs (P(SiO_2)). Cytokines were measured in homogenized lung tissue. Mean+SD, $n = 4$. $^*p<0.05$, $^{**}p<0.01$ compared with control (saline (0.9% NaCl)).

TABLE 1. Hydrodynamic Size and Zeta Potential for Aged Paint Particles and Control Paints

Paint Particle	Radius DLS (nm)	Zeta potential (mV)
P(TiO_2)	313	− 4.03 ± 2.06
P(Contr)	191	− 6.65 ± 1.27
P(Ag)	652	− 3.99 ± 2.12
P(Contr)	450	− 3.62 ± 3.52
P(SiO_2)	530	− 1.90 ± 1.69
P(Contr)	303	− 3.51 ± 0.60

in Supplementary table 4. Concentrations of Ti, Ag, and Si are higher in their respective paints compared with control paints, although concentrations are much lower than in the non-aged liquid paints (data not shown).

Mice received, under light isoflurane anesthesia, an oropharyngeal aspiration (25 μl) of particles (0.8 mg/ml) on days 0, 7, 14, 21, and 28 and were sacrificed at day 30. Concerning the pristine ENPs, a second group of mice was sacrificed at day 56.

An increase in total cells in the BAL fluid was seen in groups exposed to pristine Ag or SiO_2 ENPs, compared with the control group at day 30 (Fig. 3). Groups exposed to pristine TiO_2 ENPs or aged paint particles containing TiO_2, Ag, or SiO_2 ENPs show no increase in total cells. Differential cell counts show a limited but significant increase in neutrophils for groups exposed to pristine TiO_2, Ag, and SiO_2 ENPs at day 30, which was most pronounced in case of the pristine Ag ENPs (Fig. 3). An increase in macrophages in the pristine SiO_2 ENPs exposed group was observed as well. All groups exposed to aged paint particles containing TiO_2, Ag, or SiO_2 ENPs show no increases in neutrophils and macrophages at day 30. Cytokine analysis in lung tissue shows increases of IL-1β and KC in groups exposed to pristine Ag ENPs and aged paint particles containing TiO_2 ENPs (Fig. 4). No significant difference in IL-1β and KC was observed when comparing groups exposed to aged paint particles containing TiO_2 ENPs and aged control paint particles, indicating that the effect in the latter group was partly from the components of the control paint itself (Supplementary table 3). Concentrations of other measured cytokines (IL-12p70, IFN-γ, IL-6, IL-10, and TNF-α) were below detection limits in all groups.

Analysis of key blood parameters shows no significant changes in cell count (white blood cells, lymphocytes, neutrophils, and red blood cells) as well as for hemoglobin and hematocrit in all groups.

In Supplementary tables 5, 6, and 7, all data are summarized. The results of the second setup, in which the autopsy was performed at a later time point (day 56), show no pulmonary inflammation. When aged paints containing ENPs were compared with their proper control (aged paint without ENPs), no significant differences were observed.

Results of ENPs biodistribution are shown in Figure 5 (left graphs). An increased Ti content was found in the lung tissue at day 30 in TiO_2 ENPs-exposed mice compared with the control group (contr/d30). At day 56, Ti content was still higher compared with the control group (contr/d56), but lower than at day 30. In the liver, spleen, kidney, and heart, no significant difference in the concentration of Ti was observed. After exposure to aged paint containing TiO_2 ENPs and control paint (containing no TiO_2 ENPs, but TiO_2 pigment), a significant increase in Ti was observed in the lung (Fig. 5, right graphs). The paint containing TiO_2 ENPs caused an increase in the liver as well. Pristine Ag ENPs exposed mice show increases of Ag in the lungs at both time points (days 30 and 56), most pronounced at day 30. Significant increases of Ag in the liver, spleen, and kidney were observed as well, whereas no increases in these organs and heart were seen at day 56. Concerning Ag containing paints, no significant increase in Ag was observed in any of the studied organs. SiO_2 ENPs exposed mice show increases of Si in the lungs at both time points (days 30 and 56). An increased Si content was found in the liver at both time points as well. Mice exposed to paints containing SiO_2 or control paint showed an increased Si content in the liver at day 30.

DISCUSSION

In the present study, we evaluated the toxic effects and biodistribution of three pristine ENPs and aged paints containing ENPs after oropharyngeal aspiration in mice. We showed that the pristine ENPs have a subtle inflammatory/toxic effect in the lungs, and negligible effects on the blood parameters (systemic effects). The most pronounced effects were induced by pristine Ag ENPs in the lung as seen by an increased total and neutrophil count, and a twofold increase in pro-inflammatory cytokine secretion (KC and IL-1ß). Moreover, the aged paints containing ENPs did not modify neutrophils and only mildly induced cytokine levels. Regarding the biodistribution of the pristine ENPs Ag and Si were found outside the lung after aspiration to respectively pristine Ag and SiO_2 ENPs.

Occupational exposure to ENPs used in paints and coatings can occur during the production process, handling and application of the paint on a surface or secondary after ageing. Activities such as scratching (by children, pets), cleaning, UV exposure, drilling holes, and demolition can damage the coatings resulting in release of (nano)particles into the environment. Respiratory inhalation is the most probably route of exposure to environmental dust, however, other exposure routes such as skin and GI tract also needs to be considered as potential portals of entry (Oberdorster *et al.*, 2005).

Some studies have already been conducted on how particles incorporated in paints and coatings are released (form, composition) due to ageing processes. Kaegi *et al.* studied the facade runoff from a building painted with TiO_2 containing paint (Kaegi *et al.*, 2008). They observed that most of the TiO_2 ENPs are released as aggregates consisting of a few particles embedded in the organic binder of the paint. Göhler *et al.* showed similar results; abrasion of nano-ZnO containing coatings applied on wood or metal surfaces resulted in the release of larger matrix particles containing ZnO ENPs (Gohler *et al.*, 2010); whereas Koponen *et al.* observed no significant differences in the size distributions of dust released by sanding between paints with and without ENPs (Koponen *et al.*, 2011).

Inhalation, intratracheal instillation, and oropharyngeal aspiration are frequently used in toxicity studies to administer agents including ENPs to the respiratory tract (De Vooght *et al.*, 2009; Shvedova *et al.*, 2008). Although inhalation mimics oc-

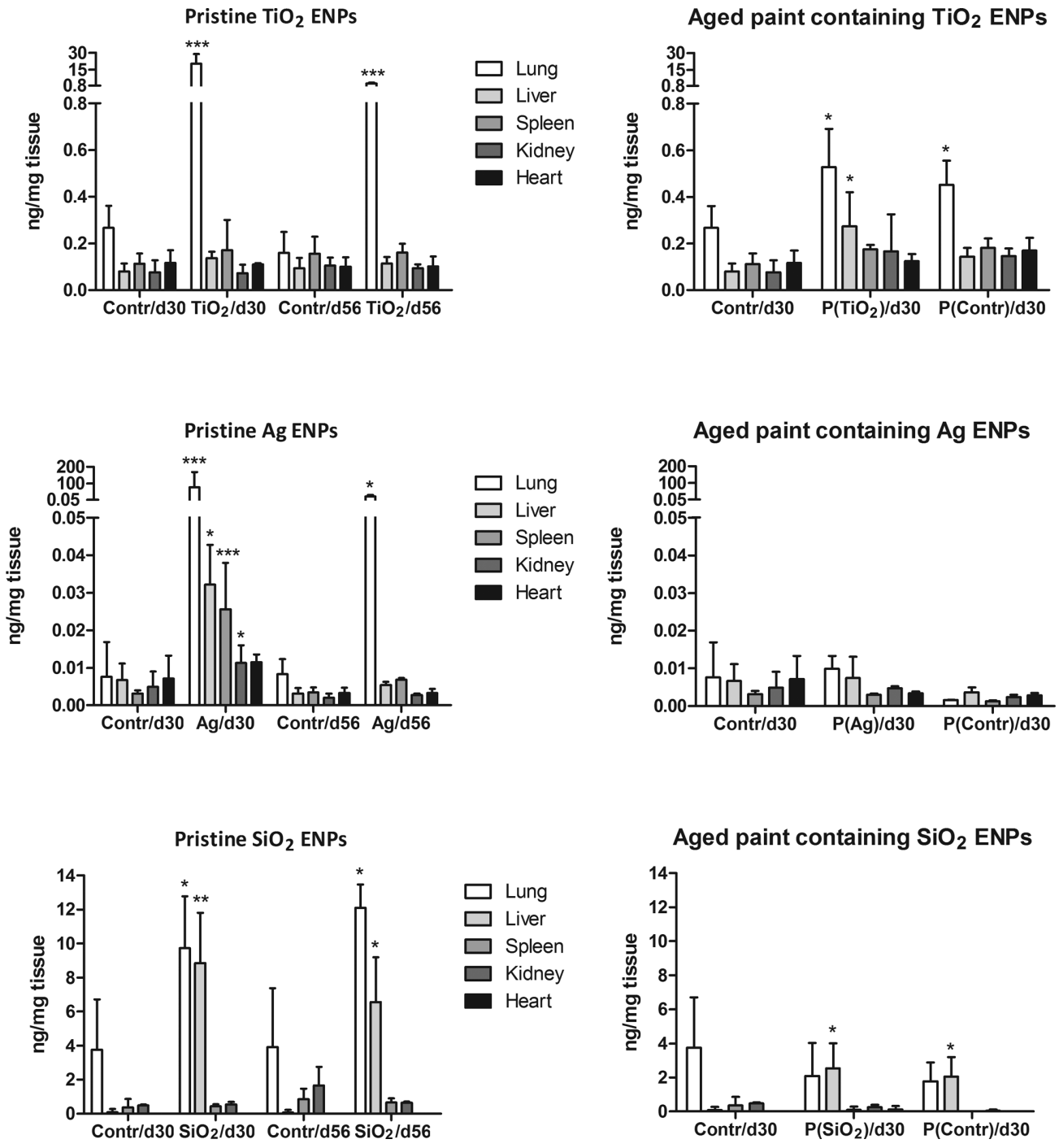

FIG. 5. Body distribution of pristine ENPs and aged paints containing ENPs to different organs. Mice were exposed to saline (controls), pristine ENPs (TiO_2, Ag, or SiO_2), aged paints containing ENPs or aged control paints without ENPs by oropharyngeal aspiration and an autopsy was performed at day 30 (d30) or day 56 (d56). Lung, liver, spleen, kidney, and heart were harvested and concentrations of Ti, Ag, or Si were determined using ICP-MS. Values are mean+SD. $^{*}p<0.05$, $^{**}p<0.01$, $^{***}p<0.001$ compared with corresponding control (saline (0.9% NaCl)).

cupational and environmental exposure the most closely, this technique requires large amounts of the test agent, is time-consuming, technically demanding, and expensive (Card *et al.*, 2008). Intratracheal instillation allows administration of exact amount of the test agent into the lung, but requires general anesthesia and can cause damage to the trachea. Oropharyngeal aspiration, the exposure technique used in this study, does not have the drawbacks of the latter and is relative easy to perform. However, a limitation is the inaccurate dose determination as part of the particles can end up in the stomach.

Despite numerous studies concerning the toxic effects of ENPs, data about ENP toxicity embedded in complex paint/coating matrices are lacking. Recently, Saber *et al.* published two studies comparing both *in vitro* and *in vivo* the toxicity of ENPs alone and when embedded in a paint matrix (Saber *et al.*, 2011, 2012). The toxicity of paint dusts with different ENPs (TiO_2,

CB, or SiO_2) was assessed *in vitro* using FE1-Muta Mouse Lung epithelial cells and *in vivo* after a single intratracheal instillation in mice. For all paints, the cytotoxicity was below 25% at a concentration of 200 μg/ml. *In vivo*, they did not observe any changes in BAL cell count (total, macrophages, neutrophils) and mRNA expression of MIP-2, MCP-1, and heme oxygenase (HO)-1 24 h after instillation of the different paint dusts. They concluded that the level of pulmonary inflammation in mice exposed to sanding dust was not affected by the addition of ENPs to paint.

Here, aged paint powder particles were generated after processing the initial liquid paints. Liquid paints were consecutively applied on a panel, dried, scratched off with a metallic spatula, milled, and finally exposed to UV-A as an ageing process. In this way, we simulate real-life situations as for example pets or children scratching walls, drilling and release after long-term exposure to UV and heat. Admittedly, in our study due to practical reasons, the UV exposure was not performed on the painted panels, but on the particles after milling. In contrast to the study of Saber *et al.* paint particles/dust were generated by sanding painted panels and no ageing process was performed (Saber *et al.*, 2012).

None of the tested paints containing TiO_2, Ag, or SiO_2 ENPs showed major pulmonary or systemic toxicity, whereas exposure to pristine ENPs induced some degree of pulmonary toxicity. These data confirm the study of Saber *et al.* (2012). Important to note is that only a small fraction of the total paint composition is composed of ENPs. Concentrations of TiO_2, Ag, and SiO_2 in the initial liquid paints are 3, 0.3, and 5%, respectively (% of total weight). ICP-MS measurements of the aged paint powders after processing from the liquid paints reveal even much lower concentrations of corresponding ENPs (TiO_2: 0.34%, SiO_2: 0.067%). In case of the paint containing Ag ENPs, almost no Ag (0.0009%) was detected in the powder paint indicating most of the Ag was removed during the processing from liquid paints to aged powder paints. The biodistribution experiments show notable distribution outside the lung of Ag to the spleen, liver, and kidney, and of Si to the liver. Ag ENPs easily dissolve and ions will cross the air-blood barrier leading to distribution to extrapulmonary organs. Based on inhalation and instillation studies, the largest part of the particles is taken up by alveolar macrophages and will be removed from the lung by respiratory mucociliary clearance (Geiser and Kreyling, 2010). Subsequently, due to swallowing they will reach the stomach and GI tract, can be taken up in the gut or will finally be excreted. Depending on the physicochemical properties of the particles, none or only a minor fraction of the particles will translocate through the air-blood barrier into the circulation and will accumulate in secondary organs (Luyts *et al.*, 2013).

In case of pristine ENPs, a second autopsy was performed at day 56 in order to investigate whether recovery took place after a longer time period. Although ENPs showed pulmonary toxic effect at the early time point (day 30), no toxicity was observed at the late time point (day 56). This indicates that the tested ENPs cause only acute toxic effects, and recovery occurs with time. Because the tested paint particles showed little to no toxicity at the early time point (day 30), from an ethical perspective, no study was performed at day 56 in this case.

In conclusion, we demonstrated that even though direct exposure to ENPs induced some toxic effects, once they were incorporated in a complex paint matrix little to no adverse toxicological effects were identified.

SUPPLEMENTARY DATA

Supplementary data are available online at http://toxsci.oxfordjournals.org/.

FUNDING

Seventh Framework Program of the European Commission NanoHouse-Grant (Agreement No. 207816); Hercules funds AKUL/11/10; Belgian Prodex Office (ESA).

ACKNOWLEDGMENT

We thank Kristin Coorevits for technical assistance with ICP-MS analyses.

REFERENCES

Card, J. W., Zeldin, D. C., Bonner, J. C. and Nestmann, E. R. (2008). Pulmonary applications and toxicity of engineered nanoparticles. *Am. J. Physiol. Lung Cell. Mol. Physiol.* **295**, L400–L411.

Chantarachindawong, R., Luangtip, W., Chindaudom, P., Osotchan, T. and Srikhirin, T. (2012). Development of the scratch resistance on acrylic sheet with basic colloidal silica (SiO2)-methyltrimethoxysilane (MTMS) nanocomposite films by sol-gel technique. *Can. J. Chem. Eng.* **90**, 888–896.

De Vooght, V., Vanoirbeek, J. A., Haenen, S., Verbeken, E., Nemery, B. and Hoet, P. H. (2009). Oropharyngeal aspiration: An alternative route for challenging in a mouse model of chemical-induced asthma. *Toxicology* **259**, 84–89.

Geiser, M. and Kreyling, W. G. (2010). Deposition and biokinetics of inhaled nanoparticles. *Part Fibre. Toxicol.* **7**, 2.

Gohler, D., Stintz, M., Hillemann, L. and Vorbau, M. (2010). Characterization of nanoparticle release from surface coatings by the simulation of a sanding process. *Ann. Occup. Hyg.* **54**, 615–624.

Hanus, M. J. and Harris, A. T. (2013). Nanotechnology innovations for the construction industry. *Prog. Mater. Sci.* **58**, 1056–1102.

Kaegi, R., Ulrich, A., Sinnet, B., Vonbank, R., Wichser, A., Zuleeg, S., Simmler, H., Brunner, S., Vonmont, H., Burkhardt, M., *et al.* (2008). Synthetic TiO2 nanoparticle emission from exterior facades into the aquatic environment. *Environ. Pollut.* **156**, 233–239.

Keller, A. A., McFerran, S., Lazareva, A. and Suh, S. (2013). Global life cycle releases of engineered nanomaterials. *J. Nanopart. Res.* **15**.

Koponen, I. K., Jensen, K. A. and Schneider, T. (2011). Comparison of dust released from sanding conventional and nanoparticle-doped wall and wood coatings. *J. Expo. Sci. Environ. Epidemiol.* **21**, 408–418.

Lee, J., Mahendra, S. and Alvarez, P. J. J. (2010). Nanomaterials in the construction industry: A review of their applications and environmental health and safety considerations. *ACS Nano* **4**, 3580–3590.

Luyts, K., Napierska, D., Nemery, B. and Hoet, P. H. M. (2013). How physico-chemical characteristics of nanoparticles cause their toxicity: Complex and unresolved interrelations. *Environ. Sci.* **15**, 23–38.

Mueller, N. C. and Nowack, B. (2008). Exposure modeling of engineered nanoparticles in the environment. *Environ. Sci. Technol.* **42**, 4447–4453.

Napierska, D., Thomassen, L. C., Rabolli, V., Lison, D., Gonzalez, L., Kirsch-Volders, M., Martens, J. A. and Hoet, P. H. (2009). Size-dependent cytotoxicity of monodisperse silica nanopar-

ticles in human endothelial cells. *Small* **5**, 846–853.

Oberdorster, G., Oberdorster, E. and Oberdorster, J. (2005). Nanotoxicology: An emerging discipline evolving from studies of ultrafine particles. *Environ. Health Perspect.* **113**, 823–839.

Saber, A. T., Jacobsen, N. R., Mortensen, A., Szarek, J., Jackson, P., Madsen, A. M., Jensen, K. A., Koponen, I. K., Brunborg, G., Gutzkow, K. B., *et al.* (2012). Nanotitanium dioxide toxicity in mouse lung is reduced in sanding dust from paint. *Part Fibre. Toxicol.* **9**, 4.

Saber, A. T., Koponen, I. K., Jensen, K. A., Jacobsen, N. R., Mikkelsen, L., Moller, P., Loft, S., Vogel, U. and Wallin, H. (2011). Inflammatory and genotoxic effects of sanding dust generated from nanoparticle-containing paints and lacquers. *Nanotoxicology.***6**,776–788.

Shvedova, A. A., Kisin, E., Murray, A. R., Johnson, V. J., Gorelik, O., Arepalli, S., Hubbs, A. F., Mercer, R. R., Keohavong, P., Sussman, N., *et al.* (2008). Inhalation vs. aspiration of single-walled carbon nanotubes in C57BL/6 mice: Inflammation, fibrosis, oxidative stress, and mutagenesis. *Am. J. Physiol. Lung Cell. Mol. Physiol.* **295**, L552–L565.

Smulders, S., Kaiser, J. P., Zuin, S., Van Landuyt, K. L., Golanski, L., Vanoirbeek, J., Wick, P. and Hoet, P. H. (2012). Contamination of nanoparticles by endotoxin: Evaluation of different test methods. *Part Fibre. Toxicol.* **9**, 41.

Som, C., Wick, P., Krug, H. and Nowack, B. (2011). Environmental and health effects of nanomaterials in nanotextiles and facade coatings. *Environ. Int.* **37**, 1131–1142.

Vorbau, M., Hillemann, L. and Stintz, M. (2009). Method for the characterization of the abrasion induced nanoparticle release into air from surface coatings. *J. Aerosol Sci.* **40**, 209–217.